Decorated DNA-Based Scaffolds as Lateral Flow Biosensors

Simone Brannetti,[a, #] Serena Gentile,[a, #] Alejandro Chamorro-Garcia,[a] Luca Barbero,[b] Erica Del Grosso*[a] and Francesco Ricci*[a]

[a] S. Brannetti, S. Gentile, Dr. A. Chamorro-Garcia, Dr. E. Del Grosso, Prof. F. Ricci
Department of Chemical Sciences and Technologies
University of Rome Tor Vergata, Via della Ricerca Scientifica, 00133, Rome, Italy
[b] RBM-Merck an affiliate of Merck KGaA, Via Ribes 1, 10010, Turin, Italy

* Corresponding authors: E-mail: erica.del.grosso@uniroma2.it; francesco.ricci@uniroma2.it
# These authors contributed equally

Supporting information for this article is given via a link at the end of the document.

Abstract: *Here we develop Lateral Flow Assays (LFAs) that employ as functional elements DNA-based structures decorated with reporter tags and recognition elements. We have rationally re-engineered tile-based DNA tubular structures that can act as scaffolds and can be decorated with recognition elements of different nature (i.e. antigens, aptamers or proteins) and with orthogonal fluorescent dyes. As a proof-of-principle we have developed sandwich and competitive multiplex lateral flow platforms for the detection of several targets, ranging from small molecules (digoxigenin, Dig and dinitrophenol, DNP), to antibodies (Anti-Dig, Anti-DNP and Anti-MUC1/EGFR bispecific antibodies) and proteins (thrombin). Coupling the advantages of functional DNA-based scaffolds together with the simplicity of LFAs, our approach offers the opportunity to detect a wide range of targets with nanomolar sensitivity and high specificity.*

Introduction

The rapid detection of biomarkers plays a crucial role in the prevention,[1,2] prognosis,[3,4] and monitoring of human disorders.[5–7] Despite significant advances have been achieved in standard laboratory based methods (i.e. ELISA, PCR), reagent-intensive and multi-step processes are often required making these approaches time consuming and costly.[8,9] Because of this there is a rising demand of platforms that allow sensitive, specific, rapid and easy-to-use measurement of diagnostic biomarkers, in point-of-care (PoC) setting.[10] Lateral Flow Assays (LFAs) respond to the above needs providing a quick, low-cost, and user-friendly approach that has found large use for diagnostic,[11,12] environmental [13–15] and food safety applications.[16,17] Numerous examples of LFAs have been demonstrated since the development of the first kit for the pregnancy self-test.[18–20] The detection of several viruses,[22–24] bacterial infections[21–24] and also multiple antibodies (i.e. IgG, IgM and IgA),[25] can be achieved by engineering specific lateral flow kits. Despite the approaches developed to date have proven sensitive and specific with also quantitative and multiplexing capabilities,[26,27] new strategies that allow to build lateral flow sensing assays with increased versatility and applicability are needed.

Synthetic DNA has recently emerged as a versatile material to build structures and devices at the nanoscale.[28–30] Numerous examples of 2D and 3D architectures with potential applications in sensing,[31–36] drug delivery[37–39] and imaging[40–43] have been described to date. DNA-based structures present several features that could be advantageous if coupled with LFAs. Synthetic DNA strands are in fact easily addressable and DNA-based structures can be decorated with different functional groups.[44–46] These may include a wide range of recognition elements and orthogonal reporter labels (i.e. fluorophores) that can be employed for the multiplexed detection of different targets.[47] Motivated by the above considerations, we propose here a novel strategy to couple the advantageous features of DNA-based structures with those of LFAs. More specifically, we have re-engineered a fluorescently-labeled DNA-based scaffold as functional reporter tag in LFA. The DNA scaffold can be decorated with optical reporter labels (i.e. fluorophores) and different recognition elements and allow the sensitive and convenient detection of multiple targets with different LF sensing formats.

Result and Discussion

In this work we have employed as DNA scaffold a model DNA structure obtained through the self-assembly of double-cross-over DNA tiles (DAE-E).[48–51] These tiles are formed through the hybridization of five different DNA strands and contain 4 single-stranded sticky ends (a, b, a', b', each of 5 nucleotides) that induce their spontaneous self-assembly into micron-scale polymeric structures.[52] To assemble our DNA scaffold, we have employed two different tiles that contain the same sticky ends and can thus co-assemble together. One tile (anchor tile) contains a DNA single-stranded overhang that can act as an anchor domain for the decoration with a recognition element (Figure 1a, S1). In the second tile (reporter tile), instead, one of the strands is covalently conjugated to a fluorophore tag (Figure 1a, S1). The DNA scaffold formed through the self-assembly of these two tiles will thus display two elements: the fluorophore and the anchor domain.[53–55] Through the simple hybridization of a modified DNA strand complementary to the anchor domain we can easily control the decoration of the DNA scaffold with different recognition elements (Figure 1b). This kind of functional scaffold can be used, for example, in a LF sandwich format (Figure 1c) in which both the scaffold and the test line of the LF strip are functionalized with a specific recognition element. In the presence of the target, the scaffold will be retained on the test line and a fluorescent band will be observed (Figure 1c).

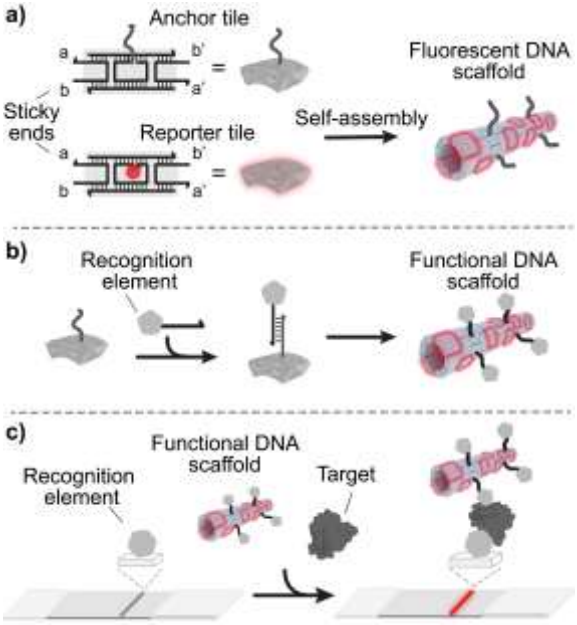

Figure 1. DNA-based scaffolds for a lateral flow test. (a) DNA tiles assembled through the hybridization of five different DNA strands displaying four sticky ends (a, b, a', b') each of five nucleotides. The tiles are re-engineered to contain either a DNA single-stranded overhang that can act as an anchor domain (anchor tile) or an optical reporter label (reporter tile). The DNA tiles are shown here as LEGO-like bricks in which knobs and holes represent the sticky ends of the tiles. DNA tiles can self-assemble into DNA scaffolds of micron-scale length. (b) Adding a modified DNA strand complementary to the anchor domain makes it possible to decorate the DNA scaffold with different recognition elements. (c) Scheme of a sandwich format of a LFA that employs functional DNA scaffolds as both reporter tags and recognition elements.

As a first step towards the use of DNA scaffolds in LFAs, we have initially characterized the signal generated by a fluorescently-labeled DNA scaffold when retained on the test line of a strip (Figure 2a). First, we have used a fluorescent microscope to confirm the successful assembly of DNA scaffolds containing different relative content of the reporter tile and anchor tile (Figures S2). In figure 2b a representative image of DNA scaffolds prepared with 90% of reporter tile and 10 % of anchor tile is reported.

We have then used a bench-top fluorescent imager to measure the signal generated on a test line displaying a capture strand complementary to the anchor strand of the DNA scaffold. A DNA scaffold with 90% of the reporter tile and 10% of the anchor tile showed an optimal signal/noise ratio with the highest tested anchor tile content and was thus employed in subsequent experiments (Figures S3). The addition of this DNA scaffold at different concentrations (from 1 to 300 nM) on the strip leads to the formation of a fluorescent band on the test line with a concentration-dependent intensity ($K_{1/2}$ = 30 ± 1 nM) (Figure 2c). Control experiments using fluorescently-labeled non-assembled monomeric tiles decorated with the anchor domain (Figure S4) do not show any fluorescent band thus supporting the hypothesis that DNA-assembled scaffolds are crucial to achieve a measurable signal (Figure 2c). Similarly, control experiments using DNA scaffolds without the anchor strand do not generate, as expected, any fluorescent band (Figure S3, ctrl).

DNA scaffolds enable multiplexed detection. To show this, we have prepared three different scaffolds each decorated with a different fluorophore and with a different anchor domain. We have immobilized the corresponding complementary capture strands of each scaffold on three different test lines of the same strip. By adding different combinations of a mixture of the DNA scaffolds we observe orthogonal signals on each test line (Figure 2d). We have also demonstrated the possibility to detect the signal generated by the fluorescently labeled DNA scaffold with smartphone camera and a UV lamp. The results are comparable in terms of sensitivity with those obtained using the bench-top imager thus further supporting the versatility of our approach and its suitability for point-of-care (Figure S5).[56]

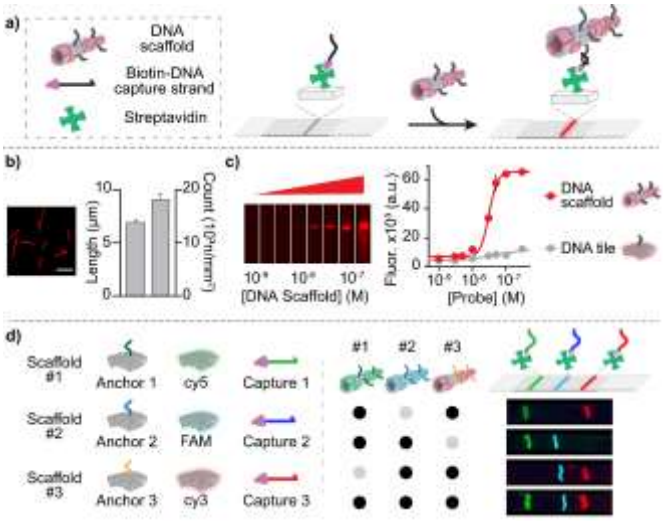

Figure 2. Characterization of functional DNA-based scaffolds for LFAs. (a) Scheme of the format assay employed to characterize the signal generated by a fluorescently-labeled DNA scaffold. (b) Fluorescence microscopy image (scale bar 5 μm) and average length and count of the assembled fluorescently-labeled DNA scaffolds (100 nM) with 90% reporter tiles and 10% anchor tile. (c) Images of the strips and fluorescent signal values of the fluorescent bands obtained at increasing concentrations of the DNA scaffolds and of monomeric tiles (DNA tile) used as control experiments. (d) Multiplexed platform obtained by adding three DNA scaffolds decorated with different fluorophores and with different anchor domains. The experiments shown in this figure were performed in 1×TAE, 12.5 mM $MgCl_2$, 0.1% Tween 20, pH 8.0. A solution containing the DNA scaffold (15 μl, 50 nM) was added on the strip and measured using a fluorescent imager after 30 min. Error bars represent standard deviations based on triplicate measurements.

After the above preliminary characterization, we have explored the possibility of using our DNA scaffolds to detect different targets, ranging from antibodies to proteins, in a sandwich-type assay. For this type of format, we have functionalized both the DNA scaffold and the strip with a recognition element specific to the target analyte. The presence of the target would thus induce the accumulation of the DNA scaffold on the test line generating a measurable fluorescent band (Figure 3a). As a first example of this format, we have developed a sandwich assay for detecting Anti-Digoxigenin antibodies (Anti-Dig antibodies). We have first functionalized the DNA scaffold with Dig by using a Dig-labeled DNA strand complementary to the anchor domain of the anchor tile (see Fig. 1b). We have also immobilized, through biotin/streptavidin interaction, a Dig-conjugated DNA duplex complex on the test line of the strip. The addition of a solution containing the Anti-Dig antibody leads to the formation of a sandwich complex on the test line that generates a fluorescent band (Figure 3a). The assay shows a concentration-dependent behavior with a $K_{1/2}$ value of 1.7 ± 0.2 nM (Figure 3b,c). Comparable results ($K_{1/2}$ =

1.5 ± 0.2 nM) were obtained using saliva samples spiked with Anti-Dig antibodies thus supporting the possibility of using our approach in complex samples (Figure 3d). We also observed limit of detection (LOD) values, calculated as the concentration of Anti-Dig giving a signal 3 times the standard deviation of the blank, of 0.6 nM and 0.7 nM for buffer and saliva, respectively. Control experiments using non-assembled monomeric tiles decorated with the anchor domain and the DNA scaffolds without the DNA strand complementary to the anchor domain do not show any measurable fluorescent band (Figure S6).

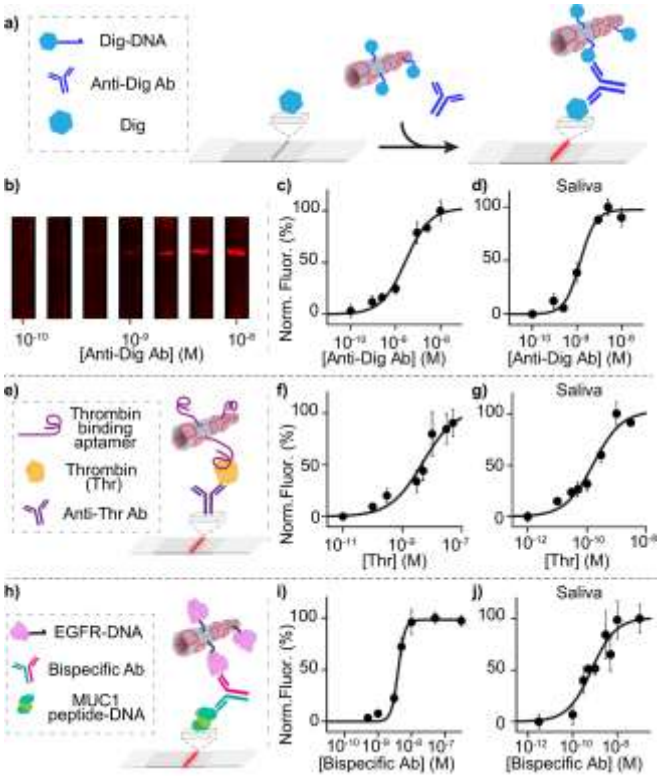

Figure 3. Sandwich LFA using DNA-based scaffolds. (a) Scheme of the sandwich assay for the detection of Anti-Dig antibodies. (b) Images of the strips and normalized fluorescent signal values obtained at increasing concentrations of Anti-Dig antibodies (c) in buffer and (d) in saliva. (e) Scheme of the sandwich assay to detect thrombin and normalized fluorescent signal values at increasing concentrations of thrombin (f) in buffer and (g) in saliva. (h) Sandwich assay for detecting Anti-MUC1/Anti-EGFR bispecific antibodies. Normalized fluorescence values at increasing concentrations of antibodies (i) in buffer and (j) in saliva. The experimental protocol for these experiments is detailed in the SI. Briefly, a solution (15 μl) of buffer or saliva spiked with different concentrations of the target antibody was added to the strip followed by the addition of a buffer solution (15 μl) containing the DNA scaffold. The fluorescent band on the test line was measured using a bench-top fluorescent imager after 30 min. Error bars represent standard deviations based on triplicate measurements.

Our approach is versatile and could be easily adapted to other targets. For example by modifying our DNA scaffold with the thrombin-binding aptamer and the strip with Anti-thrombin antibodies, we can easily detect thrombin, a protein with proteolytic activity involved in blood coagulation cascade (Figure 3e)[57]. Also in this case, the signal of the fluorescent band shows a concentration-dependent behavior ($K_{1/2}$ of 5 ± 1 nM; LOD = 0.7 nM) with comparable sensitivity in saliva samples spiked with thrombin ($K_{1/2}$ = 0.2 ± 0.1 nM; LOD = 0.05 nM) (Figure 3f,g).

The possibility of functionalizing the DNA scaffold and the LF strip with two different recognition elements allows the detection of bivalent targets with two different binding sites. For this, we have selected as target a bispecific antibody designed to bind the mucin-1 (MUC1) protein and the human epidermal growth factor receptor (EGFR) (Figure 3h). We have thus functionalized the DNA scaffold with an EGFR-conjugated DNA strand, and the test line with a DNA/PNA-chimera duplex complex, conjugated at one end with a biotin molecule and at the other end with a 15-residue peptide epitope of the MUC1 protein. The presence of the target bispecific antibody gives a concentration-dependent signal in the test line with comparable sensitivity in buffer and saliva ($K_{1/2}$ = 4.0 ± 0.1 nM, LOD = 2 nM in buffer; $K_{1/2}$ = 0.7 ± 0.3 nM, LOD = 0.3 nM in saliva) (Figure 3i,j). The platform specificity is demonstrated by testing the two monovalent antibodies (Anti-MUC1 and Anti-EGFR) that, as expected, do not show any measurable signal (Figure S7). To further explore the platform's capabilities with complex matrices, we conducted the three assays described above also in 30% serum-fortified samples and observed signals in the presence of the target even under these conditions (Figure S8). We also show that is possible to perform the sandwich assay for the detection of Anti-Dig antibodies in a single step with comparable results (Figure S9).

Figure 4. Competitive LFA for the detection of small molecules. (a) Scheme of

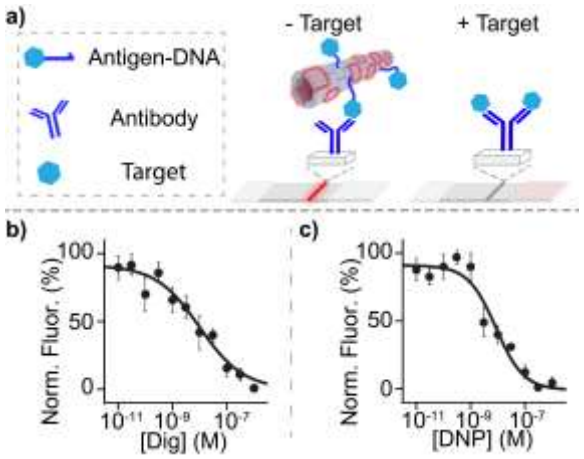

the competitive assay for the detection of small molecules. Normalized fluorescent signal values were obtained at increasing concentrations of (b) Dig and (c) 2,4-dinitrophenol (DNP). The experimental protocol for these experiments is detailed in the SI. Briefly, a solution containing the target (at the indicated concentrations) and the DNA scaffold (50 nM) were incubated for 5 minutes and then added (15 μl) to the strip. The fluorescent band on the test line was measured using a bench-top fluorescent imager after 30 min. Error bars represent standard deviations based on triplicate measurements.

DNA scaffolds also support competitive assay formats. To demonstrate this, we have decorated the scaffold with the target of interest and modified the test line with a specific recognition element. In this type of assay a competition between the analyte and the functional scaffold is established so that the presence of the target prevents the formation of a fluorescent band on the strip. In the first example, to develop a competitive assay for the detection of the small molecule digoxigenin (Dig), we have employed the same Dig-functionalized DNA scaffold described above, and we have immobilized, through adsorption mechanism, the Anti-Dig antibodies on the test line of the strip

(Figure 4a). The presence of increasing concentrations of digoxigenin leads to a decrease in the fluorescent band on the test line of the strip with a concentration-dependent behavior (Figure 4b) ($K_{1/2}$ = 10 ± 2 nM, LOD = 0.8 nM). This approach can be easily adapted to the measurement of other small molecules. For example, we have decorated the scaffold with 2,4-dinitrophenol (DNP) and the test line with Anti-DNP antibodies to detect free DNP in the solution. Also, in this case we observed a concentration-dependent signal decrease with nanomolar sensitivity ($K_{1/2}$ = 8 ± 1 nM, LOD = 2 nM) (Figure 4c).

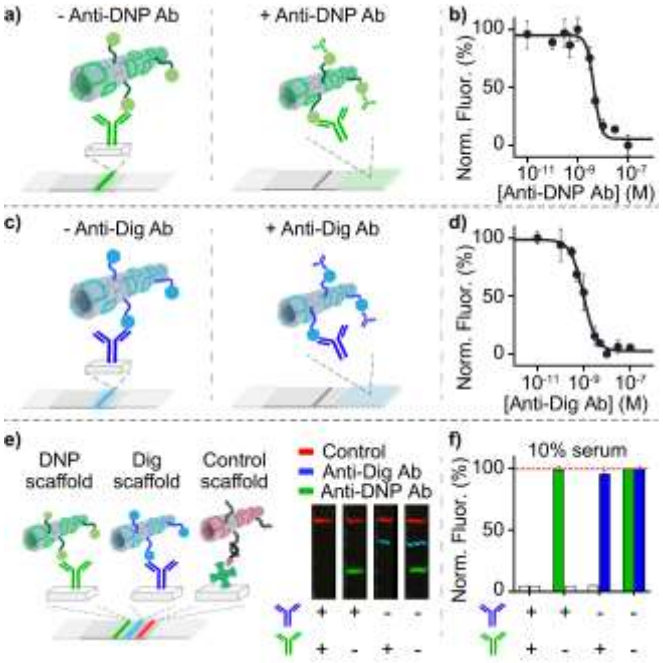

Figure 5. Competitive LFA for the detection of antibodie**s.** (a) Scheme and (b) normalized fluorescent signal values of the competitive assay for the detection of Anti-DNP antibodies. (c) Scheme and (d) normalized fluorescent signal values of the competitive assay for the detection of Anti-Dig antibodies. The results shown in this figure were obtained the same approach described in Figure 4. (e) Scheme of a multiplexed competitive assay for the simultaneous detection of Anti-DNP and Anti-Dig antibodies employing orthogonal functional DNA scaffolds. The images show the strips obtained in the presence of one or both the antibodies (30 nM) in 10% serum. (f) Bar plot representing the normalized fluorescence signal (%) in the presence of one or both the antibodies (30 nM). The red dashed line represents the fluorescence value of the control line. The experiments for the multiplexed platform were performed in 10% serum. Error bars represent standard deviations based on triplicate measurements.

We can also use the same antigen-decorated DNA scaffolds to measure target antibodies using a similar competitive format. In this case, we have immobilized on the test line the relevant antibody. The free target antibody in the sample solution would prevent the formation of the fluorescent band leading to a decrease in the observed signal. With this approach, we have detected Anti-DNP (Figure 5a,b) and Anti-Dig (Figure 5c,d) antibodies with $K_{1/2}$ values of 5.5 ± 0.5 nM and of 0.9 ± 0.1 nM, respectively and LOD values of 0.7 and 0.3 nM, respectively. Finally, thanks to the possibility of engineering multiple and orthogonal DNA scaffolds, we have developed a multiplexed competitive LFA for the simultaneous detection of Anti-DNP and Anti-Dig antibodies. To do this, we have employed orthogonal DNA scaffolds modified with three different fluorophores and orthogonal anchor domains (Figure S10). We have then modified three different test lines, the first with Anti-DNP antibodies, the second with Anti-Dig antibodies, and the third test line (control line) with a DNA capture strand (Figure 5e). As expected, the presence of a single antibody prevents the fluorescent band on the corresponding test line, and only in the presence of both antibodies none of the two test lines shows a fluorescent band (Figures 5e,f, S11).

Furthermore, to demonstrate the suitability of this platform in point-of-care settings, we performed the same competitive assay shown in figure 5c (for the detection of Anti-Dig antibodies) using a camera smartphone and a portable UV lamp. With this set-up we obtained comparable $K_{1/2}$ (2.1 ± 0.2 nM vs 0.9 ± 0.1 nM) and LOD values (0.9 nM vs 0.3 nM) (Figure S12).

Conclusion

Here we have demonstrated a proof-of-principle method for the use of DNA-based structures as both reporter tags and recognition elements in LFAs. The DNA structures used in this work are easily assembled and can be decorated with different recognition elements and signaling labels providing a high affinity recognition of the target of interest and an amplified fluorescent signal on the LF strip. We have demonstrated that DNA scaffolds can be used to detect antibodies, proteins, and small molecules in both sandwich and competitive assay formats, with sensitivities comparable to those obtained in conventional LFAs.[58-59]

Despite the maturity of LFA technology, some limitations still affect its widespread use in some applications.[60] We argue that the use of DNA-based structures in LFAs can provide interesting opportunities to overcome these limitations and to provide an alternative to the use of gold nanoparticles for novel and more versatile LFA platforms. For example, DNA-based structures can provide an easier to control conjugation of the recognition element compared to gold nanoparticles. Moreover, we show here that it is straightforward to label the DNA scaffolds with different fluorescent labels thus supporting the possibility of expanding the range of colors (signals) used in LFAs. This, together with the orthogonality of DNA-DNA interactions can allow multiplexing capabilities that are currently difficult to achieve with traditional LFAs.

Acknowledgements

This work was supported by the European Research Council, ERC (project no. 819160) (F.R.), Associazione Italiana per la Ricerca sul Cancro, AIRC (project no. 21965) (F.R.), the Italian Ministry of University and Research (Project of National Interest, PRIN, 2017YER72K), and the European Union's Horizon 2020 research and innovation program under the Marie Skłodowska-Curie grant agreement No 896962, "ENZYME-SWITCHES" (E.D.G.) and No. 799332, "Smart BioSense" (A.C-G.).

Keywords: DNA Nanotechnology • DNA structures• Lateral flow assays • DNA sensors • Antibodies

[1] C. Dincer, R. Bruch, A. Kling, P. S. Dittrich, G. A. Urban, *Trends Biotechnol* **2017**, *35*, 728–742.

[2] Y. Liu, L. Zhan, Z. Qin, J. Sackrison, J. C. Bischof, *ACS Nano*

2021, *15*, 3593–3611.
[3] J. Li, J. Macdonald, *Biosens Bioelectron* **2016**, *83*, 177–192.
[4] Z. Wang, J. Zhao, X. Xu, L. Guo, L. Xu, M. Sun, S. Hu, H. Kuang, C. Xu, A. Li, *Small Methods* **2022**, *6*, 2101143.
[5] L. Yang, K. D. Patel, C. Rathnam, R. Thangam, Y. Hou, H. Kang, K. Lee, *Small* **2022**, *18*, 2104783.
[6] Y. Xue, X. Feng, X. Fan, G. Zhu, J. McLaughlan, W. Zhang, X. Chen, *Small Struct* **2022**, *3*, 2100096.
[7] Y. Tian, L. Ma, M. Gong, G. Su, S. Zhu, W. Zhang, S. Wang, Z. Li, C. Chen, L. Li, L. Wu, X. Yan, *ACS Nano* **2018**, *12*, 671–680.
[8] H.-S. Huang, C.-L. Tsai, J. Chang, T.-C. Hsu, S. Lin, C.-C. Lee, *Clinical Microbiology and Infection* **2018**, *24*, 1055–1063.
[9] E. Engvall, *Clin Chem* **2010**, *56*, 319–320.
[10] P. Brangel, A. Sobarzo, C. Parolo, B. S. Miller, P. D. Howes, S. Gelkop, J. J. Lutwama, J. M. Dye, R. A. McKendry, L. Lobel, M. M. Stevens, *ACS Nano* **2018**, *12*, 63–73.
[11] A. Kodjo, C. Calleja, M. Loenser, D. Lin, J. Lizer, *Biomed Res Int* **2016**, *2016*, 1–3.
[12] J. H. Soh, H.-M. Chan, J. Y. Ying, *Nano Today* **2020**, *30*, 100831.
[13] P. Li, Q. Zhang, W. Zhang, *TrAC Trends in Analytical Chemistry* **2009**, *28*, 1115–1126.
[14] D. Quesada-González, G. A. Jairo, R. C. Blake, D. A. Blake, A. Merkoçi, *Sci Rep* **2018**, *8*, 16157.
[15] D. Du, J. Wang, L. Wang, D. Lu, Y. Lin, *Anal Chem* **2012**, *84*, 1380–1385.
[16] L. Anfossi, C. Baggiani, C. Giovannoli, G. D'Arco, G. Giraudi, *Anal Bioanal Chem* **2013**, *405*, 467–480.
[17] H. Sohrabi, M. R. Majidi, P. Khaki, A. Jahanban-Esfahlan, M. Guardia, A. Mokhtarzadeh, *Compr Rev Food Sci Food Saf* **2022**, *21*, 1868–1912.
[18] A. Rubio-Monterde, D. Quesada-González, A. Merkoçi, *Anal Chem* **2022**, DOI 10.1021/acs.analchem.2c04529.
[19] C. Pereira, C. Parolo, A. Idili, R. R. Gomis, L. Rodrigues, G. Sales, A. Merkoçi, *Trends Chem* **2022**, *4*, 554–567.
[20] Anders O. GrubbUlla C. Glad, *Immunoassay with Test Strip Having Antibodies Bound Thereto*, **1976**.
[21] D. Wang, S. He, X. Wang, Y. Yan, J. Liu, S. Wu, S. Liu, Y. Lei, M. Chen, L. Li, J. Zhang, L. Zhang, X. Hu, X. Zheng, J. Bai, Y. Zhang, Y. Zhang, M. Song, Y. Tang, *Nat Biomed Eng* **2020**, *4*, 1150–1158.
[22] B. Ince, M. K. Sezgintürk, *TrAC Trends in Analytical Chemistry* **2022**, *157*, 116725.
[23] B. D. Grant, C. E. Anderson, J. R. Williford, L. F. Alonzo, V. A. Glukhova, D. S. Boyle, B. H. Weigl, K. P. Nichols, *Anal Chem* **2020**, *92*, 11305–11309.
[24] J. G. Peter, A. Haripesad, L. Mottay, S. Kraus, R. Meldau, K. Dheda, American Thoracic Society, **2011**, pp. A5313–A5313.
[25] I. Montesinos, D. Gruson, B. Kabamba, H. Dahma, S. Van den Wijngaert, S. Reza, V. Carbone, O. Vandenberg, B. Gulbis, F. Wolff, H. Rodriguez-Villalobos, *Journal of Clinical Virology* **2020**, *128*, 104413.
[26] A. Sena-Torralba, R. Álvarez-Diduk, C. Parolo, A. Piper, A. Merkoçi, *Chem Rev* **2022**, *122*, 14881–14910.
[27] C. Parolo, A. Sena-Torralba, J. F. Bergua, E. Calucho, C. Fuentes-Chust, L. Hu, L. Rivas, R. Álvarez-Diduk, E. P. Nguyen, S. Cinti, D. Quesada-González, A. Merkoçi, *Nat Protoc* **2020**, *15*, 3788–3816.
[28] M. Rossetti, E. Del Grosso, S. Ranallo, D. Mariottini, A. Idili, A. Bertucci, A. Porchetta, *Anal Bioanal Chem* **2019**, *411*, 4293–4302.
[29] E. Del Grosso, P. Irmisch, S. Gentile, L. J. Prins, R. Seidel, F. Ricci, *Angewandte Chemie International Edition* **2022**, *61*, DOI 10.1002/anie.202201929.
[30] P. Wang, T. A. Meyer, V. Pan, P. K. Dutta, Y. Ke, *Chem* **2017**, *2*, 359–382.
[31] A. Porchetta, A. Vallée-Bélisle, K. W. Plaxco, F. Ricci, *J Am Chem Soc* **2013**, *135*, 13238–13241.
[32] S. Ranallo, A. Amodio, A. Idili, A. Porchetta, F. Ricci, *Chem. Sci.* **2016**, *7*, 66–71.
[33] S. Bracaglia, S. Ranallo, F. Ricci, *Angewandte Chemie International Edition* **2023**, DOI 10.1002/anie.202216512.
[34] J. Bucci, P. Irmisch, E. Del Grosso, R. Seidel, F. Ricci, *J Am Chem Soc* **2022**, *144*, 19791–19798.
[35] M. Rossetti, S. Brannetti, M. Mocenigo, B. Marini, R. Ippodrino, A. Porchetta, *Angewandte Chemie* **2020**, *132*, 15083–15088.
[36] M. Rossetti, R. Ippodrino, B. Marini, G. Palleschi, A. Porchetta, *Anal Chem* **2018**, *90*, 8196–8201.
[37] S. Sellner, S. Kocabey, K. Nekolla, F. Krombach, T. Liedl, M. Rehberg, *Biomaterials* **2015**, *53*, 453–463.
[38] J. Mikkilä, A.-P. Eskelinen, E. H. Niemelä, V. Linko, M. J. Frilander, P. Törmä, M. A. Kostiainen, *Nano Lett* **2014**, *14*, 2196–2200.
[39] P. K. Lo, P. Karam, F. A. Aldaye, C. K. McLaughlin, G. D. Hamblin, G. Cosa, H. F. Sleiman, *Nat Chem* **2010**, *2*, 319–328.
[40] Y.-X. Zhao, A. Shaw, X. Zeng, E. Benson, A. M. Nyström, B. Högberg, *ACS Nano* **2012**, *6*, 8684–8691.
[41] H. Pei, N. Lu, Y. Wen, S. Song, Y. Liu, H. Yan, C. Fan, *Advanced Materials* **2010**, *22*, 4754–4758.
[42] V. P. Ma, K. Salaita, *Small* **2019**, *15*, 1900961.
[43] E. Del Grosso, L. J. Prins, F. Ricci, *Angewandte Chemie International Edition* **2020**, *59*, 13238–13245.
[44] L. N. Green, H. K. K. Subramanian, V. Mardanlou, J. Kim, R. F. Hariadi, E. Franco, *Nat Chem* **2019**, *11*, 510–520.
[45] N. C. Seeman, H. F. Sleiman, *Nat Rev Mater* **2018**, *3*, 17068.
[46] D. Y. Zhang, R. F. Hariadi, H. M. T. Choi, E. Winfree, *Nat Commun* **2013**, *4*, 1965.
[47] S. Ranallo, D. Sorrentino, F. Ricci, *Nat Commun* **2019**, *10*, 5509.
[48] P. W. K. Rothemund, *Nature* **2006**, *440*, 297–302.
[49] T. J. Fu, N. C. Seeman, *Biochemistry* **1993**, *32*, 3211–3220.
[50] E. Winfree, F. Liu, L. A. Wenzler, N. C. Seeman, *Nature* **1998**, *394*, 539–544.
[51] A. Heuer-Jungemann, T. Liedl, *Trends Chem* **2019**, *1*, 799–814.
[52] R. Ibusuki, T. Morishita, A. Furuta, S. Nakayama, M. Yoshio, H. Kojima, K. Oiwa, K. Furuta, *Science (1979)* **2022**, *375*, 1159–1164.
[53] S. Gentile, E. Del Grosso, L. J. Prins, F. Ricci, *Angewandte Chemie International Edition* **2021**, *60*, 12911–12917.
[54] S. Gentile, E. Del Grosso, P. E. Pungchai, E. Franco, L. J. Prins, F. Ricci, *J Am Chem Soc* **2021**, *143*, 20296–20301.
[55] N. Farag, M. Đorđević, E. Del Grosso, F. Ricci, *Advanced Materials* **2023**, *35*, DOI 10.1002/adma.202211274.
[56] S. K. Biswas, S. Chatterjee, S. Bandyopadhyay, S. Kar, N. K. Som, S. Saha, S. Chakraborty, *ACS Sens* **2021**, *6*, 1077–1085.
[57] A. Pasternak, F. J. Hernandez, L. M. Rasmussen, B. Vester, J. Wengel, *Nucleic Acids Res* **2011**, *39*, 1155–1164.
[58] C. Parolo, A. de la Escosura-Muñiz, A. Merkoçi, *Biosens. Bioelectron.* **2013**, *40*, 412-416.
[59] H. Xu, X. Mao, Q. Zeng, S.Wang, A. Kawde, G.Liu, *Anal. Chem.* **2009**, *81*, 2, 669–675.
[60] H. de Puig, I. Bosch, L. Gehrke, K. Hamad-Schifferli 4, *Trends in Biotechnol.*. **2017**, *35*, 1169.

Table of Contents

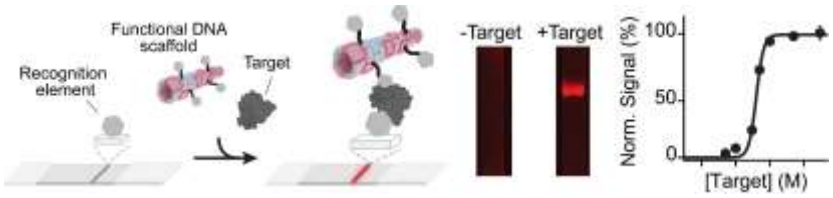

Here we have developed Lateral Flow Assays that employ as functional elements DNA-based structures decorated with reporter tags and recognition elements. With these analytical platforms we have demonstrated the rapid, sensitive and quantitative detection of several targets including small molecules, antibodies and proteins.